Pflügers Arch - Eur J Physiol (2001) 441:629–638
DOI 10.1007/s004240000471

ORIGINAL ARTICLE

F. Franciolini · R. Hogg · L. Catacuzzeno · A. Petris
C. Trequattrini · D.J. Adams

Large-conductance calcium-activated potassium channels in neonatal rat intracardiac ganglion neurons

Received: 10 June 2000 / Received after revision: 14 September 2000 / Accepted: 16 October 2000 / Published online: 28 November 2000

Abstract The properties of single Ca^{2+}-activated K^+ (BK) channels in neonatal rat intracardiac neurons were investigated using the patch-clamp recording technique. In symmetrical 140 mM K^+, the single-channel slope conductance was linear in the voltage range –60/+60 mV, and was 207±19 pS. Na^+ ions were not measurably permeant through the open channel. Channel activity increased with the cytoplasmic free Ca^{2+} concentration ($[Ca^{2+}]_i$) with a Hill plot giving a half-saturating $[Ca^{2+}]$ ($K_{0.5}$) of 1.35 µM and slope of ≅3. The BK channel was inhibited reversibly by external tetraethylammonium (TEA) ions, charybdotoxin, and quinine and was resistant to block by 4-aminopyridine and apamin. Ionomycin (1–10 µM) increased BK channel activity in the cell-attached recording configuration. The resting activity was consistent with a $[Ca^{2+}]_i$ <100 nM and the increased channel activity evoked by ionomycin was consistent with a rise in $[Ca^{2+}]_i$ to ≥0.3 µM. TEA (0.2–1 mM) increased the action potential duration ≅1.5-fold and reduced the amplitude and duration of the afterhyperpolarization (AHP) by 26%. Charybdotoxin (100 nM) did not significantly alter the action potential duration or AHP amplitude but reduced the AHP duration by ≅40%. Taken together, these data indicate that BK channel activation contributes to the action potential and AHP duration in rat intracardiac neurons.

Keywords Action potential · Afterhyperpolarization · Charybdotoxin · Intracellular calcium · Parasympathetic neurons · Tetraethylammonium ions

R. Hogg · D.J. Adams (✉)
Department of Physiology and Pharmacology,
University of Queensland, Brisbane, QLD 4072 Australia
e-mail: dadams@plpk.uq.edu.au
Fax: +61-7-33654933

F. Franciolini · L. Catacuzzeno · A. Petris · C. Trequattrini
Dipartmento Biologia Cellulare e Molecolare,
Universita' di Perugia, Via Pascoli 1, 06100 Perugia, Italy

Introduction

In central and peripheral neurons, action potentials are followed by an afterhyperpolarization (AHP) lasting from tens of millisecond to several seconds. The AHPs have been shown to be due to the activation of Ca^{2+}-activated K^+ conductance(s) following Ca^{2+} influx via depolarization-activated Ca^{2+} channels during the action potential. In mammalian sympathetic neurons, at least three classes of Ca^{2+}-dependent K^+ currents have been identified according to their kinetics and pharmacology [1, 4, 37]. In rat superior cervical ganglion neurons, the Ca^{2+}-dependent K^+ current is voltage dependent and is comprised of two components with distinct activation kinetics [4, 35]. Two of these currents are involved in the generation and shape of the AHP, the principal class of which has been termed $I_{K,Ca1}$ or I_{AHP}. This current functions primarily to repolarize the membrane from the peak of the action potential. $I_{K,Ca1}$ in sympathetic ganglion cells from rat and guinea-pig [4, 19, 23] is blocked by nanomolar concentrations of apamin. A second, slow Ca^{2+}-dependent K^+ current, $I_{K,Ca2}$, is found in some sympathetic neurons [7, 19] exhibiting a long afterhyperpolarization (LAH). This current is voltage insensitive and its activation is secondary to either Ca^{2+} influx or release from internal stores. $I_{K,Ca2}$ is blocked by agents such as ryanodine which inhibit Ca^{2+} mobilization from intracellular stores, but is insensitive to apamin and tetraethylammonium (TEA).

The only class of Ca^{2+}-activated K^+ channel in mammalian autonomic neurons categorized according to its unitary conductance is a large-conductance (≅200 pS; BK or maxi K) Ca^{2+}-dependent K^+ channel [17, 41]. This large-conductance Ca^{2+}-dependent K^+ channel is activated by an elevation of the cytoplasmic free Ca^{2+} concentration and is modulated by membrane potential. The macroscopic current corresponding to activation of BK channels is termed I_C and has been shown to be blocked by TEA ions and the scorpion toxin charybdotoxin (ChTX) [20]. It is largely on the basis of the effects of TEA and ChTX on the repolarization phase of the ac-

tion potential and AHP, that BK channels have been suggested to regulate the shape of the action potential and neuronal firing behaviour.

In neonatal and adult rat intracardiac neurons, the Ca^{2+}-dependent K^+ current ($I_{K,Ca}$) accounts for approximately one-third of the total outward K^+ current [45, 46]. The action potential repolarization is not affected by the Ca^{2+} channel blocker, Cd^{2+}, but the magnitude and duration of the AHP are reduced in the presence of either Cd^{2+} or Ca^{2+}-free external solutions [45, 46]. Superfusion of Ca^{2+}-free solutions has been reported to cause a small membrane depolarization in rat intracardiac neurons [40] and it has been suggested that $I_{K,Ca}$ may contribute to the resting membrane potential.

The aim of the present study is to characterize the Ca^{2+}-dependent K^+ channels, their contribution to the action potential and AHP in the soma membrane of rat intracardiac neurons and to assess the ability of these channels in cell-attached membrane patches to monitor changes in the submembrane Ca^{2+} concentration. A preliminary report of some of these results has been presented to the Società Italiana di Fisologia [42].

Materials and methods

Cell preparation

Parasympathetic neurons from neonatal rat intracardiac ganglia were isolated and cultured as described previously [46]. Briefly, 2- to 8-day-old rats were stunned and decapitated, the hearts were excised and placed in a saline solution containing (in mM): 140 NaCl; 3 KCl; 2.5 $CaCl_2$; 0.6 $MgCl_2$; 7.7 glucose and 10 histidine, (pH 7.2). The atria were separated and the medial region containing the pulmonary veins and superior vena cava was identified, isolated and incubated in the above saline solution, containing 1 mg ml^{-1} collagenase (Type 2, activity ≅200 units mg^{-1}, Worthington Biochemical, Freehold, N.J., USA). Following enzyme digestion, the ganglia were removed and neurons were dispersed by trituration in a high-glucose culture medium [Dulbecco's modified Eagle media, containing 10% (v/v) fetal calf serum, 100 units/ml penicillin and 0.1 mg ml^{-1} streptomycin], using a fire-polished Pasteur pipette. The dissociated neurons were plated on to laminin-coated 18-mm glass coverslips and incubated at 37°C in a 95% air:5% CO_2 atmosphere for 24–60 h. For experimentation, coverslips containing dissociated neurons were transferred to a perfusion chamber (0.5 ml volume) mounted on an inverted microscope and individual cells were identified under 400× magnification using phase-contrast optics.

Electrophysiological recording

Single-channel recordings were made using the cell-attached, outside- and inside-out configurations of the patch-clamp technique [18]. Pipettes were pulled from borosilicate glass (Hilgemberg, Malsfeld, Germany) using a PUL-100 pipette puller (WPI, Sarasota, Fla., USA) and following fire polishing had resistances of 10–15 MΩ, corresponding to an estimated tip area of about 0.5–0.8 µm [38]. Single-channel currents were recorded using a List L/M EPC-7 patch-clamp amplifier (List-Electronic, Darmstadt, Germany). Voltage protocols were applied using pClamp software (Version 5.5, Axon Instruments, Foster City, Calif., USA). Signals were filtered at 1 kHz then digitized at 10 kHz (Digidata 1200 interface, Axon Instruments) and stored on the hard disc of a PC (Pentium, 100 MHz) for viewing and analysis. Current-clamp recordings were made using the amphotericin B-perforated patch whole-cell recording configuration and conventional dialysed whole-cell configuration, recordings were made using an Axopatch 200A patch-clamp amplifier (Axon Instruments). Data were filtered at 10 kHz and digitized at 60 kHz.

Solutions and drugs

Bath solution was a physiological salt solution (PSS) containing (in mM): 140 NaCl; 3 KCl; 2.5 $CaCl_2$; 2 $MgCl_2$; 7.7 glucose and 10 MOPS (pH 7.2). In inside-out experiments the cytoplasmic side of the patch was perfused with a solution containing (in mM): 130 KCl; 1 $MgCl_2$; 10 MOPS and 1 EGTA-K. $CaCl_2$ was added at the concentration necessary to obtain the desired free Ca^{2+} concentration using a dissociation constant for Ca-EGTA at pH 7.2 of 10^{-7} M. The same solution was used to fill the pipette in outside-out experiments. The pipette solution for inside-out and cell-attached experiments was the PSS solution. For whole-cell perforated-patch recording the pipette solution contained: 75 K_2SO_4; 55 KCl; 5 $MgSO_4$; 10 HEPES; titrated to pH 7.2 with *N*-methyl-D-glucamine and 240 µg ml^{-1} amphotericin B (Sigma). For dialysed whole-cell recording the pipette solution contained: 140 KCl; 2 MgATP; 1 EGTA; 10 HEPES-KOH; 0.2 MgGTP; pH 7.2. All chemicals used were of analytical grade. Ionomycin (Sigma) was bath applied.

Data analysis

The open probability of the channel was calculated from amplitude histograms of 60-s recordings in which only a single channel was present. The presence of only one active channel in the patch was verified by preliminary recording at positive potentials and high [Ca^{2+}]. The clampfit program (Axon Instruments, ver. 5.5) was used to fit the histograms with Gaussian curves.

The duration of open and closed intervals was measured by using the 50% threshold method [9] and the events were binned according to the logarithm of their duration [25]. The resulting distributions of open and closed events were fitted with the sum of exponential functions and the minimum number of components was estimated by the maximum likelihood method [25]. An additional exponential component was considered significant when the increase in the logarithm of the likelihood obtained was >3. To reduce the possibility of detecting "phantom" exponential components in the kinetic analysis, the events with a duration shorter than twice the dead time of our system (230 µs, measured as the minimal duration of a detected square-wave current) were excluded from the fitting. Stability plots were constructed as described by McManus and Magleby [27]. Briefly, the mean durations of groups of 50 sequential open intervals were measured for a continuous recording of about 5000 open events and plotted against sequential interval number. Data are expressed as mean ±SEM.

Results

Ionic selectivity and conductance

Excised outside- and inside-out membrane patches contained an average number of three to four active large-conductance (BK) channels in the patch. The large-conductance channels were studied in >100 excised membrane patches; however, the presence of other types of Ca^{2+}-activated K^+ channels cannot be excluded. Although a small-conductance K^+-selective channel was observed occasionally (n<10 patches), further experiments to test its Ca^{2+} dependence were not undertaken. Some membrane patches contained a smaller channel

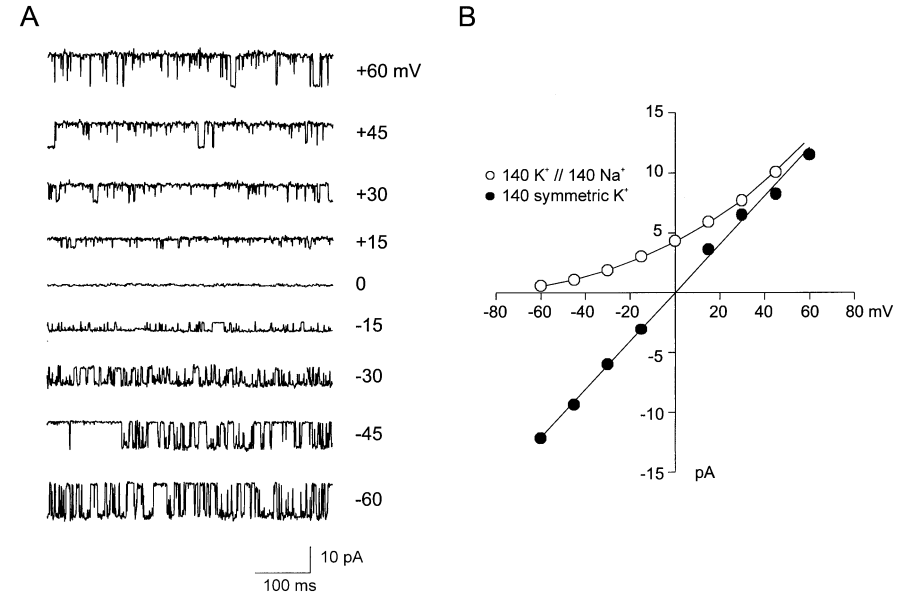

Fig. 1A, B Unitary Ca^{2+}-dependent K^+ currents in rat parasympathetic neurons. **A** Representative single-channel traces recorded from an outside-out membrane patch in symmetrical 140 mM K^+ at the indicated membrane potentials. **B** Unitary current–voltage relationship for a single Ca^{2+}-activated K^+ channel recorded from an outside-out patch in symmetrical 140 mM K^+ (●), and in external 140 mM Na^+ (3 mM K^+) and internal 140 mM K^+ (○) (*140 Na^+//140 K^+*). The composition of the bath and pipette solutions are given in Materials and methods. Free intracellular $[Ca^{2+}]$ was 3 µM. Single-channel conductance in symmetrical conditions was linear in the voltage range –60 to +60 mV, and data points could be well fitted by a *line*. The slope conductance resulting from the best fit of the data was 202 pS. Experimental points obtained in asymmetrical conditions (○), interpolated with a polynomial function, did not display a clear reversal potential

poorly selective for K^+ versus Na^+, and Ca^{2+} insensitive, that could be easily recognized by its flickering kinetics.

Representative single-channel traces obtained at the indicated membrane voltages in symmetrical 140 mM K^+ are shown in Fig. 1A. Unitary currents were obtained in the presence of 3 µM Ca^{2+} intracellularly. Figure 1B shows a typical current–voltage (*I–V*) curve obtained from an outside-out patch in either symmetrical 140 mM K^+, or in 140 mM $[K^+]_i$ and 140 mM $[Na^+]_o$. The *I–V* plot obtained in symmetrical conditions did not exhibit any rectification in the range –60/+60 mV. Only when depolarizations >+80 mV were applied was a reduction in channel conductance observed (data not shown). Best linear fit of the data gave a slope conductance of 202 pS and the average single-channel conductance was 207±19 pS (n=7). Replacing 140 mM K^+ with 140 mM Na^+ plus 3 mM K^+, the *I–V* relation became non-linear and a clear reversal potential could not be measured at hyperpolarized potentials as the current became asymptotic to the abscissa. The single-channel conductance was highly variable in different patches and in asymmetrical conditions the unitary current amplitude at 0 mV varied in the range 4.2–4.9 pA.

Ca^{2+} and voltage dependence

The open probability (P_{open}) of the BK channel was dependent both on membrane potential and $[Ca^{2+}]_i$. To assess the dependence of P_{open} on both of these parameters, two series of experiments were carried out in which P_{open} was measured first as a function of Ca^{2+} concentration at a fixed potential (0 mV), and then as function of membrane potential at three different $[Ca^{2+}]_i$ (0.1, 1 and 3 µM). These experiments were carried out with 140 mM internal K^+ and external Na^+ (plus 3 mM K^+). Figure 2A shows representative single-channel traces recorded at a membrane potential of 0 mV from inside-out patches exposed at the indicated $[Ca^{2+}]_i$. Open probabilities obtained from these experiments did not approach unity, even for $[Ca^{2+}]_i$ higher than 10 µM since the channel activity was occasionally interrupted by long closures lasting several seconds. These long closed states have been reported previously and interpreted as inactivated [3] or Ca^{2+}-blocked [24] states. More recently, it has been proposed that they are due to BK channel block by Ba^{2+} ions contaminating the solution [12]. Therefore, these long inactive periods (>2 s) are ignored in the analysis of the Ca^{2+} and voltage dependence of the channels since they probably do not represent the intrinsic gating behaviour of the channel. Under these conditions, the measured P_{open} at different $[Ca^{2+}]_i$ ranged from 0 to 1 and were distributed according to the Hill equation. Figure 2B plots the average P_{open} from several neurons as function of $[Ca^{2+}]_i$. P_{open} was calculated from amplitude histograms of 60-s-long single-channel recordings at 0 mV. Best fit of the data with the equation $P_{open}=1/\{1+(K_{0.5}/[Ca^{2+}])^n\}$ gave a $K_{0.5}$ of 1.35 µM and a Hill coefficient of 3.1, indicative of multiple Ca^{2+}-binding sites.

The voltage dependence of the BK channel is illustrated in Fig. 2C which shows P_{open} plotted as a function of membrane potential for three different cells exposed to $[Ca^{2+}]_i$ of 0.3, 1 and 3 µM, respectively. The range of

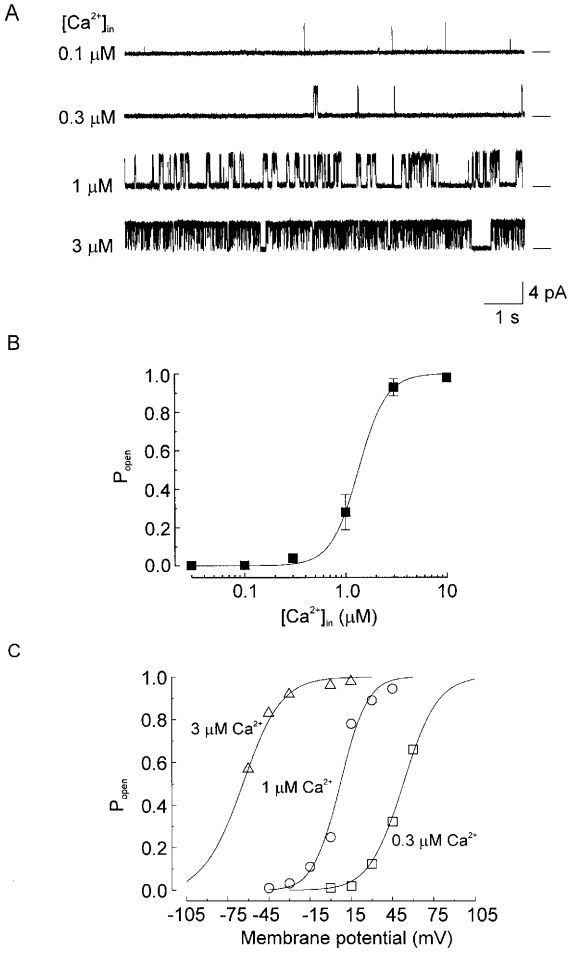

Fig. 2A–C Ca^{2+} and voltage dependence of K^+ channel open probability. **A** Single-channels traces recorded from an inside-out patch containing a single active channel, exposed to the indicated concentrations of intracellular free Ca^{2+}. Internal and external solutions contained 140 mM K^+ and 140 mM Na^+ as the main cations. Membrane potential was held at 0 mV. **B** Open probability (P_{open}, 0 mV) is plotted as a function of intracellular Ca^{2+} concentration. Data points, representing averaged values from three to five channels (mean ±SEM), were fitted with the equation $P_{open}=1/\{1+(K_{0.5}/[Ca^{2+}])^n\}$, yielding a value of 1.35 μM for the half-saturating $[Ca^{2+}]$, $K_{0.5}$, and 3.1 for the Hill coefficient, n. P_{open} at the varying Ca^{2+} concentrations was determined from the amplitude histograms constructed from 60-s-long single-channel recordings. In determining the P_{open}, closures longer than 2 s were ignored (see text). **C** Plot of P_{open} as a function of membrane potential for three channels exposed to the indicated intracellular Ca^{2+} concentrations, respectively. Amplitude histograms, used to assess the P_{open} at different voltages, were constructed from 60-s traces recorded from outside-out patches containing only one active channel. Data points were fitted to Boltzmann distributions using the equation $P_{open}=1/[1+\exp(V_{1/2}-V)/V_{e\text{-}fold}]$, where $V_{1/2}$ is the half-activation potential and $V_{e\text{-}fold}$ is the potential (in mV) necessary for an e-fold change in P_{open}. $V_{1/2}$ values of 53, 7 and –64 mV, and $V_{e\text{-}fold}$ of 11, 8.2 and 12.8 were obtained for $[Ca^{2+}]_i$ of 0.3, 1 and 3 μM, respectively. Internal solution contained 140 mM K^+ and external 140 mM Na^+ as the predominant cations

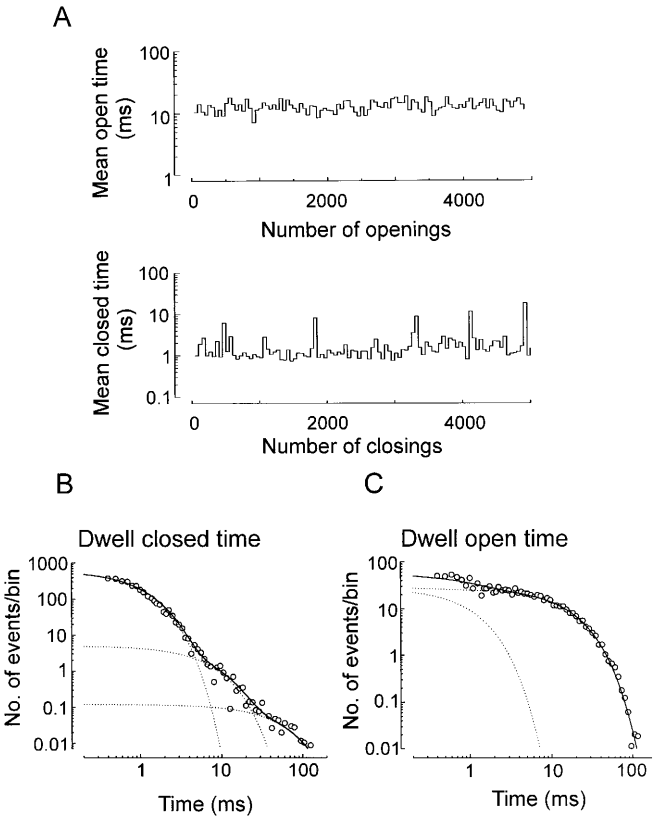

Fig. 3A–C Steady-state kinetics of single Ca^{2+}-dependent K^+ channels in rat parasympathetic neurons. **A** Stability plot of mean durations of successive openings (*upper plot*) and closings (*lower plot*) throughout a continuous single-channel recording. Groups of 50 sequential open or closed events were averaged and plotted against the number of openings for 5000 consecutive single-channel openings. **B** Dwell time histogram for the closed state, plotted on log–log co-ordinates, obtained from the same single-channel recording utilized for the stability plot in **A**. The *continuous line* represents the best fit, obtained by the method of maximum likelihood, which is the sum of three exponential components with time constants (and areas) of: 0.85 ms (94%), 5.66 ms (5.2%) and 42.6 ms (0.9%). The *dashed lines* represent the single exponential components for open and closed distributions. **C** Dwell time histogram for the open state from the same recording as in **B**. *Continuous line* is the best fitted sum of two exponential components with time constants (and areas) of: 13.9 ms (94%) and 0.9 ms (6%)

Ca^{2+} concentrations was selected so that, in the voltage range examined (–60/+60 mV), an adequate set of data to be fitted with Boltzmann distributions could be collected. Although the use of symmetrical K^+ conditions might have been more convenient to determine P_{open}, particularly at negative potentials, we used physiological ionic conditions. Furthermore, it has been reported that variations in the concentration of some ionic species and in particular external K^+, may significantly alter the P_{open} of the channel [32]. Lower or higher Ca^{2+} concentrations than those used induced a channel activity too close to either 0 or 1 at any test voltage, respectively, to preclude an adequate fit. Fit of the data relative to the three cells shown in Fig. 2C produced half-maximal activation potentials of +53, +7 and –64 mV, and slope factors (expressed as mV/e-fold) of 11, 8.2 and 12.8 respectively for $[Ca^{2+}]_i$ of 0.3, 1 and 3 μM. As done previously, long closures (>2 s) that occurred mostly when strong depolarizations were applied were ignored for the analysis.

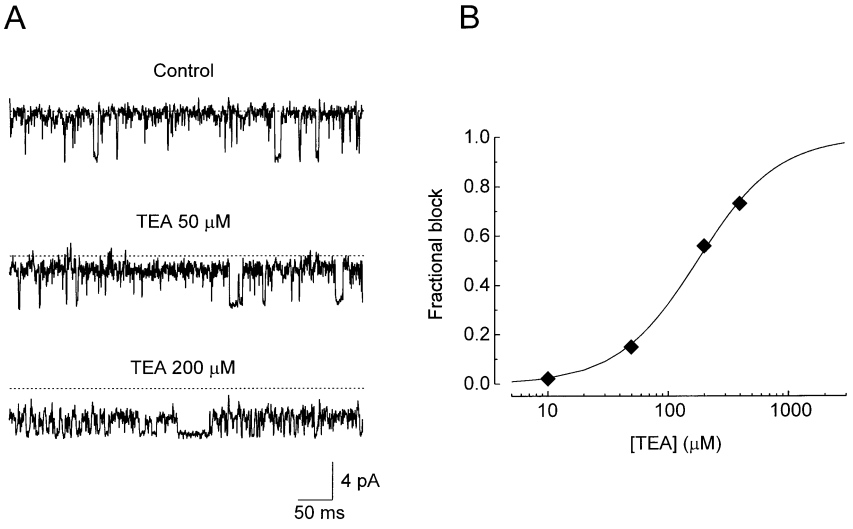

Fig. 4A, B Block of Ca^{2+}-dependent K^+ channel by external TEA. **A** Single-channel traces obtained from an outside-out patch in external 140 mM Na^+ and internal 140 mM K^+ in control conditions, and after perfusion with 50 and 200 μM TEA. Currents were filtered at 1 kHz (–3 dB, 4 pole Bessel filter). Note the reduction in current amplitude after addition of TEA. The *dashed lines* above the *traces*, representing the control current amplitude, are drawn for comparison. **B** Current amplitudes in the presence of external TEA (indicated as fractional block) are plotted against TEA concentration. Best fit of the data with the Hill equation yielded a $K_{0.5}$ of 180 μM and molecularity of 1.2

Steady-state kinetics

A 70-s-long single-channel recording at 0 mV was used to analyse the steady-state kinetics of the BK channel. Since BK channels have been shown to exhibit changes in kinetic behaviour, shifting between different modes of activity in a variety of preparations [27], we first examined the kinetic stability of the BK channel. To look for possible different kinetic modes in the behaviour of the channel and to test its stability over time, the mean durations of groups of sequential open and closed intervals were plotted against sequential interval number to form stability plots [27]. Figure 3A shows a typical stability plot of mean durations for groups of 50 consecutive open and closed intervals for a continuous recording of about 5000 open events. Mean open and closed times fluctuate about the overall mean of 12.7 ms and 1.48 ms, respectively, for all the recording, maintaining relatively low deviations from these values. The larger variability of the mean closed time compared to the open time stability plot is an indication of the presence of many closed states in the kinetic scheme of the channel. These plots indicate that the BK channel is kinetically stable over time, and its properties can be analysed by using the Markovian model [8]. Furthermore, the minimum number of kinetic states necessary to describe the channel behaviour was determined by plotting the dwell time distributions for open and closed states and determining the exponential components needed to reproduce these distributions. Figure 3B, C present the dwell time distributions in a double logarithmic plot obtained from the same single-channel recording used to construct the stability plot. The open circles plot the experimental observations (≅5000 for each plot) and the continuous line represents the best fit obtained using the method of maximal likelihood [9, 27]. With our experimental resolution (dead time 230 μs) we could determine a minimum of two and three exponential components for the open and closed states, respectively, in this single-channel recording. Very long closures of several seconds were also present in the single-channel recording from which the closed dwell time plot was constructed. However, because of their rare occurrence, the area of this component was too small to obtain an accurate fit.

Blockade by external TEA ions

To define a pharmacological profile of the channel, the effects of several K^+ channel inhibitors were tested. External application of TEA at micromolar concentrations reduced the apparent single-channel current amplitude, which was accompanied by an increase in channel flickering. A similar effect, previously observed in rat sympathetic neurons [41], is consistent with a mechanism of block where block and unblock rate constants of TEA are too fast to be fully resolved. That is, the reduction in single-channel current is only an artefact of the low-pass filter and the sampling rate used in the digitization of the data [6, 47]. According to this view, the amplitude of single-channel current measured in the presence of the drug depends on the ratio between the mean residence time for the open-blocked and unblocked states of the channel. Unitary current traces in control conditions and in the presence of 50 and 200 μM of TEA are shown in Fig. 4B. These records clearly show that the TEA-induced current reduction is associated with increased channel flickering. The single-channel current amplitude measured in the presence of varying blocker concentrations (see Fig. 4A) can be used to determine the efficacy of block through a dose–response curve. In Fig. 4B a

graph is shown in which the single-channel current, normalized to the control value, is plotted as function of TEA concentration. Figure 4B shows that at TEA concentrations higher than 400 μM, the single-channel current becomes too small to be measured, whereas a concentration of 180 μM is necessary to reduce the current by ≅50% of its control value. Data points, fitted according to the equation $I_{TEA}/I_{con}=1/(1+[TEA]^n/K_{0.5})$ yielded a Hill coefficient of 1.2.

Sensitivity to K^+ channel toxins and drugs

The efficacy of ChTX and apamin was tested on the BK channel. The channel was blocked by nanomolar concentrations of ChTX but not by apamin (up to 1 μM). A representative single-channel current recording is shown in Fig. 5A in control conditions, and following bath application of 1 nM ChTX (arrow). Addition of the ChTX strongly reduced the P_{open} of the channel and fractioned the activity in bursts. Within a burst, however, the kinetics of the channel did not show obvious differences. The effect of the toxin was totally reversible after prolonged washout. These data are consistent with the block mechanism proposed by Miller et al. [28] in which the toxin reversibly blocks the channel by binding to it in a bimolecular fashion with very slow rate constants. Given that the mechanism of ChTX block of K^+ channels is supported by substantial evidence [21, 28], and given the large amount of data required for a rigorous test of its validity, only two of the several predictions that this model allows were tested. In particular, we verified that addition of ChTX did not induce modification of the intraburst kinetics of the channel, and that by increasing the toxin concentration only the burst duration (inversely related to the product $k_{on}\cdot$[ChTX]) decreased, whereas the interburst duration (only related to k_{off} and not depending on [ChTX]) remained unaffected (data not shown).

The effect of externally applied quinine on single BK channel activity was also examined. Quinine block has the typical features of open-channel block, namely it induces a flickering behaviour and reduces the current amplitude at higher concentrations. Representative single-channel traces, shown in Fig. 5B, were recorded from an excised outside-out patch in control conditions and in the presence of 50 μM quinine extracellularly. At this concentration, quinine not only induces the characteristic flickering, but also reduces the apparent single-channel conductance.

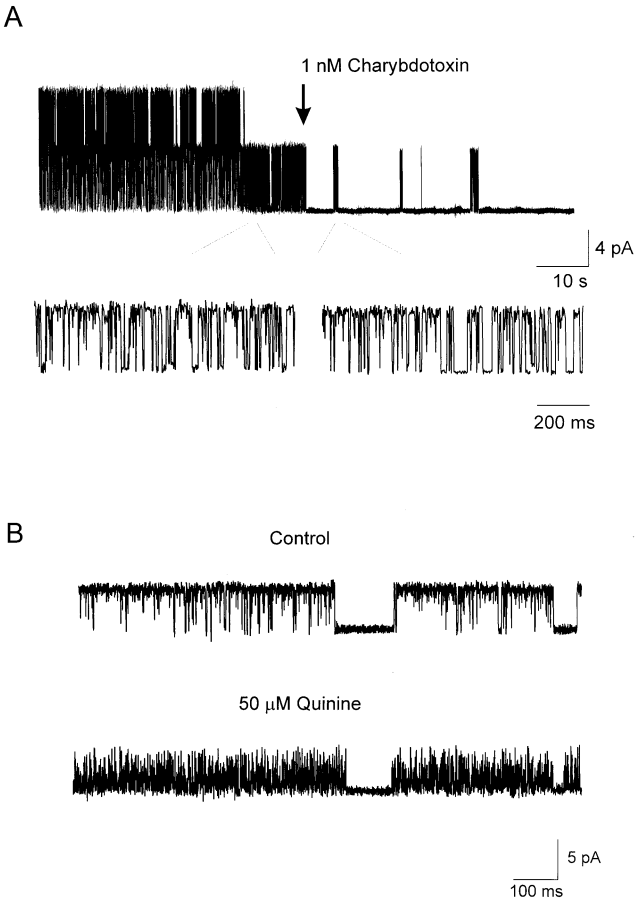

Fig. 5A, B Charybdotoxin and quinine inhibition of Ca^{2+}-dependent K^+ channels. **A** The *upper trace* shows ≅100 s of single-channel recording from an outside-out patch containing two active channels, before and after addition of 1 nM charybdotoxin (*ChTX*). In presence of the toxin, the activity of the channel is strongly reduced and the channel opens only in brief bursts. The *lower traces* show on an expanded time scale the activity of the channel in control conditions and within a burst in the presence of the toxin. Note that ChTX does not affect the kinetics of the channel, but only induces long periods of inactivity, consistent with a block mechanism where the drug binds and unbinds to the channel with very slow rate constants. Membrane potential was 0 mV and internal and external solution contained 140 mM K^+ and 140 mM Na^+, respectively. Free internal [Ca^{2+}] was 3 μM. **B** Control traces at 0 mV recorded from two different outside-out patches with internal and external solutions containing 140 mM K^+ (free Ca^{2+} 3 μM) and 140 mM Na^+, respectively. The effects of addition of external quinine (50 μM) are shown below. A pronounced increase in channel flickering is evident and at the quinine concentration used a significant reduction in current amplitude can also be observed due to incomplete resolution of single events caused by the fast block and unblock rate constants

Activation of BK channels in cell-attached patches by ionomycin

A series of experiments was carried out using the cell-attached recording configuration to demonstrate the use of the BK channel as a probe for changes in submembrane $[Ca^{2+}]_i$. In a typical experiment, unitary currents were initially recorded under control conditions to verify that the BK channel was present, its activity compatible with the physiological $[Ca^{2+}]_i$, and its kinetics stable over time. The activity of the same channel was then recorded after bath application of ionomycin which raises $[Ca^{2+}]_i$ through influx of Ca^{2+} across the plasma membrane. In Fig. 6A, C, representative unitary currents are shown, together with the relative amplitude histograms, obtained in control conditions from a cell-attached patch

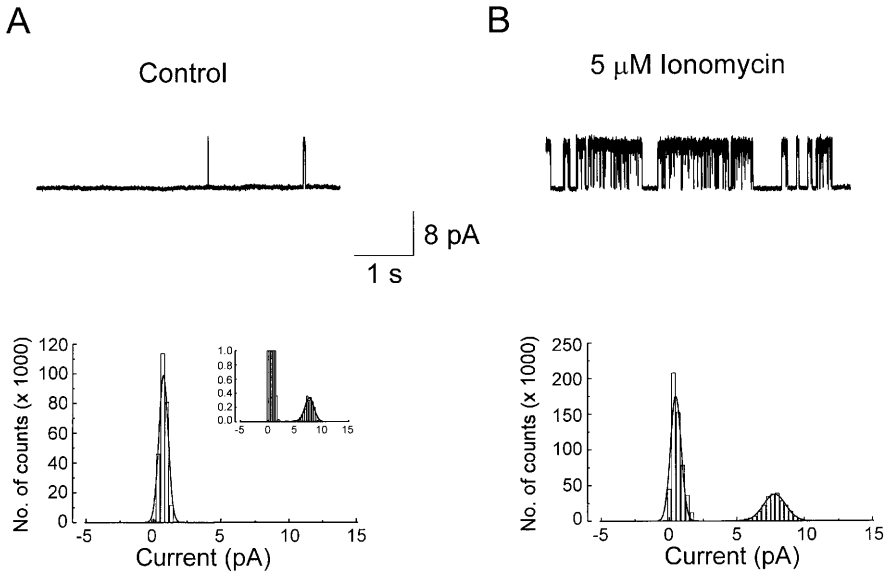

Fig. 6A, B Effects of bath application of ionomycin to cell-attached membrane patches. **A** Representative single-channel trace, with relative amplitude histogram (constructed from a 60-s recording), obtained from a cell-attached patch, with pipette and bath solutions containing 140 mM K^+ and 140 mM Na^+, respectively. Pipette potential was held at +120 mV, corresponding to an effective membrane voltage of approximately +50 mV. The *inset* shows an expanded part of the amplitude histogram to make the closed-state peak visible. **B** Single-channel trace and histogram from the same patch as in **A**, after 1 min from the beginning of perfusion of the cell with 5 μM ionomycin. The open probability of the channel increased from 0.008 in control conditions to 0.31 in the presence of ionomycin

held at +120 mV (estimated membrane potential ≅–50 mV). As indicated by the amplitude histograms, the channel activity was very low, (P_{open}<0.1) and compatible with a $[Ca^{2+}]_i$ lower than 0.1 μM.

Addition of 5 μM ionomycin induced a large increase in channel activity, evident both from the traces and the amplitude histograms of Fig. 6B, D. The increase in channel activity evoked by ionomycin is consistent with a $[Ca^{2+}]_i$ of about 0.3 μM (see Fig. 2C), which is slightly lower than that reported to be present in human T lymphocytes [44]. Open probabilities measured in the presence of 5 μM ionomycin, from two 120-s single-channel recordings, were 0.31 and 0.27, respectively, compared to the corresponding control values of 0.008 and 0.013 obtained in the absence of ionomycin. Single-channel activity was highly variable during drug application, suggesting that the Ca^{2+} level in microdomains may change significantly with time. The effects of ionomycin could not be reversed even after several minutes of washout, suggesting that after the cytoplasm is exposed to large amounts of Ca^{2+} ions, the buffering capacity of the cell may be compromised.

BK channel contribution to the action potential and AHP

The effects of the K^+ channel inhibitors ChTX, iberiotoxin, apamin and TEA on action potential configuration and AHP were investigated in isolated neurons from rat intracardic ganglia using the perforated-patch whole-cell recording technique. The membrane potential was held at either –60 or –50 mV under current-clamp conditions and single action potentials were evoked by depolarizing current pulses of 500 pA for 2 ms. In neurons held at –60 mV, the control action potential amplitude and duration at 0 mV were 112.1±2.1 mV and 1.60±0.5 ms (*n*=28), respectively. The mean AHP amplitude was –12.6±0.5 mV (*n*=28) and reversed at approximately –90 mV, close to the K^+ equilibrium potential. The duration of the AHP was highly variable ranging from approximately 50 to 250 ms, reflecting the heterogeneity of the intracardiac ganglion neuron population [2, 13, 40]. Apamin (1 μM, *n*=4), iberiotoxin (100 nM, *n*=6) and ChTX (100 nM, *n*=6) had no significant effects on the amplitude or duration of the action potential. TEA (200 μM) had the most profound effect on the action potential (Fig. 7A), whereby the action potential amplitude was increased to 1.13±0.1 (*n*=5) times control and its duration at 0 mV was increased 1.46±0.2-fold (*n*=5). In neurons held at –50 mV, the AHP amplitude (–17.1±0.6 mV, *n*=14) was slightly but not significantly reduced in the presence of 100 nM ChTX (*n*=7; *P*>0.05) but the duration of the AHP in all neurons studied was reduced by 40±6% (*n*=7; *P*<0.01) (Fig. 7B). In contrast, the amplitude of the AHP was reduced by 26±3% (*n*=9) upon bath application of TEA (0.2–1 mM). Inhibition of Ca^{2+} influx through depolarization-activated Ca^{2+} channels with bath application of 100 μM Cd^{2+} reversibly decreased the AHP amplitude by 34±5% (*n*=3; Fig. 7C) similar to that observed in the presence of TEA.

Discussion

In the present study, we have described the biophysical and pharmacological properties of the large-conductance, Ca^{2+}-dependent K^+ (BK) channels in soma mem-

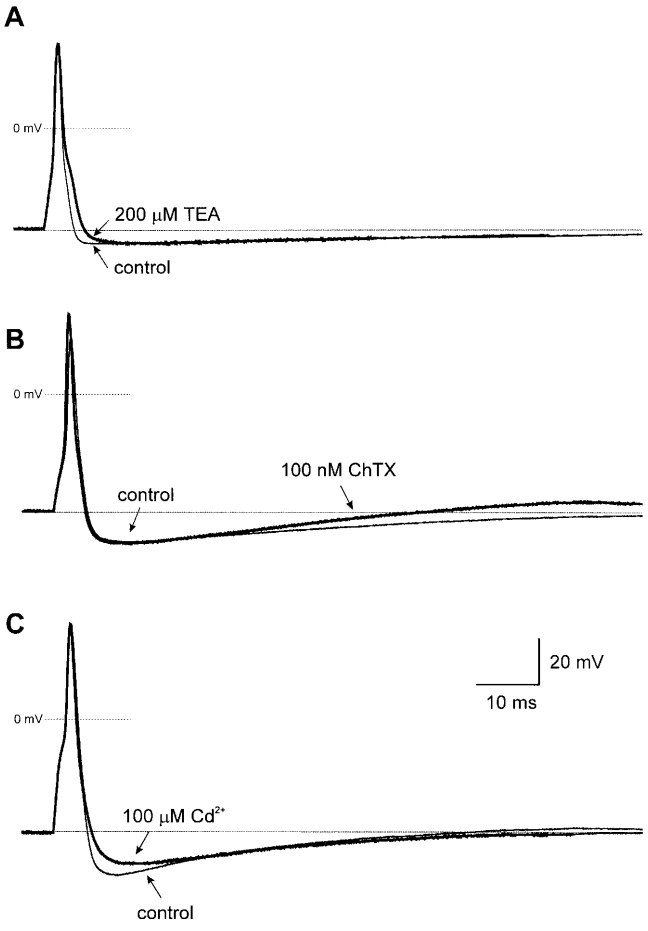

Fig. 7A–C Effect of the Ca^{2+}-activated K^+ channel inhibitors TEA and charybdotoxin (*ChTX*) and the Ca^{2+} channel blocker Cd^{2+} on the action potential and afterhyperpolarization. Resting membrane potential was held at –50 mV under current-clamp conditions and action potentials were elicited by brief depolarizing current pulses (500 pA, 2 ms). Action potentials were obtained in the absence (control) and presence of either 200 μM TEA (**A**), 100 nM charybdotoxin (**B**) or 100 μM Cd^{2+} (**C**), bath applied

brane of neonatal rat intracardiac neurons. BK channels were activated by both membrane depolarization and an increase in $[Ca^{2+}]_i$. Each of the four α-subunits that form the BK channel is made of two functional parts: a transmembrane domain including the voltage sensor, and an extended tail containing the intracellular Ca^{2+} binding domain [39]. The single-channel conductance of 207±19 pS in symmetrical 140 mM K^+ solutions is similar under the same ionic conditions to values reported for BK channels in rat sympathetic neurons (≅200 pS) [41], rabbit coeliac neurons (180–220 pS) [17], rat motoneurons (214 pS) [36] and rat hippocampal neurons (220 pS) [14]. As observed for other BK channels, the channel was selective for K^+ ions, and Na^+ ions were not measurably permeant through the open channel. The membrane potentials for half-maximal activation of the BK channel were +53 mV, +7 mV and –64 mV for 0.3, 1 and 3 μM internal Ca^{2+}, respectively. Therefore, a tenfold increase in $[Ca^{2+}]_i$ produced a negative shift of the activation curve by >100 mV. Occasionally the BK channel entered very long closed states lasting several seconds, the probability of which increased with depolarization and $[Ca^{2+}]_i$. These long closed states have been reported previously and were initially interpreted as inactivated [3] or Ca^{2+}-blocked [24] states of the channel. More recently, however, they have been shown to result from state-dependent block by Ba^{2+} present as a contaminant in the experimental solutions [12].

The BK channel P_{open} increased as a function of $[Ca^{2+}]_i$ accordingly with a $K_{0.5}$ of 1.3 μM and Hill coefficient of ≅3. This Ca^{2+} sensitivity is consistent with that observed in most neuronal preparations; however, it is about one order of magnitude smaller (the $K_{0.5}$ about tenfold higher) than that found in vascular smooth muscle cells [5]. The lower Ca^{2+} affinity of neuronal BK channels appears to be due to the lack of the β-subunit that smooth muscle cells have associated with the α-subunit in a 1:1 stoichiometry [15]. The β-subunit has in fact a marked effect on BK channel activity, decreasing up to tenfold the $[Ca^{2+}]_i$ to obtain half-maximal activation of the channel [15, 26, 31]. Open and closed time distributions, determined from analysis of steady-state kinetics of the channel, were fitted by the sum of two and three exponential functions, respectively, indicative of multiple open and closed states. Given the resolution of our recording system and the number of open and closed intervals included in the analysis, this result is consistent with the kinetic analysis of the BK channels in rat skeletal muscle [27].

The BK channel was inhibited reversibly by external TEA (10–500 μM), ChTX (1–100 nM), and quinine (1–100 μM) and was resistent to block by 4-aminopyridine (1–3 mM) and apamin (0.1–1 μM). TEA applied either internally or externally has been shown to inhibit the Ca^{2+}-dependent K^+ channel with complete block occurring at 1 mM and 5 mM TEA, respectively [41]. Ca^{2+}-dependent K^+ currents (I_C) in mammalian autonomic neurons have also been reported to be inhibited by external application of Ba^{2+} (1–10 mM), ChTX (10–100 nM), and quinine (10–200 μM) [16] but were insensitive to 4-aminopyridine (1–10 mM).

Bath application of ionomycin (1–10 μM) to stimulate Ca^{2+} influx increased BK channel activity in the cell-attached recording configuration. The resting activity was consistent with a $[Ca^{2+}]_i$ <100 nM, as evaluated from experiments in excised patches, and the increased channel activity evoked was consistent with a rise in $[Ca^{2+}]_i$ to ≥0.3 μM. It has been recently argued, however, that the Ca^{2+} dependence of the BK channel P_{open} as obtained from excised patches cannot be used as a reference curve for estimating the $[Ca^{2+}]_i$ in intact cells, since BK channels in contact with the intact cytoplasm show a Ca^{2+} dependence markedly different to that in excised conditions [30]. In particular, the Hill coefficient which in studies from excised patches ranges around 3–4 [43] was approximately 8 in intact cells. Given such a high Hill coefficient, the P_{open} of the BK channel would increase from 0.1 to 0.9 with a $[Ca^{2+}]_i$ increase from 1.0 to

1.6 µM (given a $K_{0.5}$ of 1.3 µM). Under these conditions, the BK channel would not be a useful Ca^{2+} probe. However, in the study by Muñoz et al. [30], the P_{open} was determined under non-stationary conditions, i.e. $[Ca^{2+}]_i$ varied continuously, although slowly, during the experiment. It is therefore necessary to verify these results by constructing the Ca^{2+} activation curve of the BK channel (i.e. P_{open} versus $[Ca^{2+}]_i$) in intact cells under stationary conditions.

Functional significance

Although BK channels have an intrinsic voltage sensitivity, their function is to hyperpolarize the cell following a burst of action potentials or single action potentials of sufficient duration to raise cytoplasmic Ca^{2+} levels. Macroscopic Ca^{2+}-activated K^+ currents (I_C) have been studied in rat sympathetic and parasympathetic ganglion neurons [1]. Activation of I_C contributes to action potential repolarization and the AHP: blockade of I_C by TEA or ChTX slows action potential repolarization and reduces the fast AHP in a number of neuronal preparations [1, 37]. The increase in action potential duration and inhibition of AHP amplitude by TEA and AHP duration by ChTX are consistent with BK channels contributing to the action potential repolarization and AHP. The differential effects of TEA and ChTX on the AHP characteristics suggest that more than one type of Ca^{2+}-activated K^+ channel underlies the AHP in rat intracardiac neurons.

The precise source of Ca^{2+} for BK channel activation remains unclear, except for the notion that Ca^{2+} entry through voltage-gated Ca^{2+} channels would activate them. Inhibition of Ca^{2+} influx through voltage-gated Ca^{2+} channels by extracellular Cd^{2+} reduced the AHP amplitude but did not appreciably affect the action potential or AHP duration in neonatal rat intracardiac neurons. Cd^{2+} block of the TEA-sensitive (ChTX-insensitive), fast AHP but not the ChTX-sensitive, slow AHP suggests that Ca^{2+} influx may not be necessary for activation of the BK channels underlying the slow AHP. Investigations of the activity of Ca^{2+}-activated K^+ channels in cell-attached patches in hippocampal neurons show that the BK channel is selectively activated by N-type Ca^{2+} channels, whereas the small-conductance Ca^{2+}-activated K^+ (SK) channels, whose activation underlies the slow AHP, is activated by Ca^{2+} influx through L-type Ca^{2+} channels [22, 29]. These observations support the concept of submembrane Ca^{2+} microdomains and the co-localization of voltage-dependent Ca^{2+} and Ca^{2+}-activated K^+ channels, to explain the specificity of coupling between ion channels, and avoidance of cross-talking among specific cellular processes. Entry of Ca^{2+} can activate selectively the BK but not the SK channels, and vice versa, in spite of the comparable Ca^{2+} sensitivity of the two types of Ca^{2+}-activated K^+ channels [11, 33]. Given the steep relationship between BK channel activation and $[Ca^{2+}]_i$, modulation of Ca^{2+} influx and consequently of the $[Ca^{2+}]_i$ at the active sites could effectively contribute to the shape of the action potential, AHP and firing behaviour through modulation of the BK conductance [10, 34]. Further studies are required to examine the sources of Ca^{2+} underlying the activation of the BK channels contributing to the fast (TEA-sensitive) and slow (ChTX-sensitive) AHP in neonatal rat intracardiac neurons.

Acknowledgements This work was supported by the National Health and Medical Research Council of Australia Grant 961138 (to D.J.A.) and Grant 92.689.CT04 from Italian Consiglio Nazionale Ricerch (to F.F.).

References

1. Adams DJ, Harper AA (1995) Electrophysiological properties of autonomic ganglion neurons. In: McLachlan EM (ed) The autonomic nervous system, Vol. 6. Autonomic ganglia. Harwood Academic, London, pp 153–212
2. Allen TGJ, Burnstock G (1987) Intracellular studies of the electrophysiological properties of cultured intracardiac neurones of the guinea-pig. J Physiol (Lond) 388:349–366
3. Barrett JN, Magleby KL, Pallotta BS (1982) Properties of single calcium-activated potassium channels in cultured rat muscle. J Physiol (Lond) 331:211–230
4. Belluzzi O, Sacchi O (1990) The calcium-dependent potassium conductance in rat sympathetic neurones. J Physiol (Lond) 422:561–583
5. Benham CD, Bolton TB, Lang RJ, Takewaki T (1986) Calcium-activated potassium channels in single smooth muscle cells of rabbit jejunum and guinea-pig mesenteric artery. J Physiol (Lond) 371:45–67
6. Blatz AL, Magleby KL (1984) Ion conductance and selectivity of single calcium-activated potassium channels in cultured rat muscle. J Gen Physiol 84:1–23
7. Cassell JF, McLachlan EM (1987) Two calcium-activated potassium conductances in a subpopulation of coeliac neurones of guinea pig and rabbit. J Physiol (Lond) 394:331–349
8. Colquhoun D, Hawkes AG (1995) The principles of the stochastic interpretation of ion-channel mechanisms. In: Sakmann B, Neher E (eds) Single channel recording, 2nd edn. Plenum, New York, pp 397–482
9. Colquhoun D, Sigworth FJ (1995) Fitting and statistical analysis of single-channel records. In: Sakmann B, Neher E (eds) Single channel recording, 2nd edn. Plenum, New York, pp 483–587
10. Crest M, Gola M (1993) Large conductance Ca^{2+}-activated K^+ channels are involved in both spike shaping and firing regulation in Helix neurones. J Physiol (Lond) 468:174–191
11. Davies PJ, Ireland DR, McLachlan EM (1996) Sources of Ca^{2+} for different Ca^{2+}-activated K^+ conductances in neurones of the rat superior cervical ganglion. J Physiol (Lond) 495: 353–366
12. Diaz F, Wallner M, Stefani E, Toro L, Latorre R (1996) Interaction of internal Ba^{2+} with a cloned Ca^{2+}-dependent K^+ (hslo) channel from smooth muscle. J Gen Physiol 107:399–407
13. Edwards FR, Hirst GDS, Klemm MF, Steele PA (1995) Different types of ganglion cells in the cardiac plexus of guinea-pigs. J Physiol (Lond) 486:453–471
14. Franciolini F (1988) Calcium and voltage dependence of single Ca^{2+}-activated K^+ channels from cultured hippocampal neurons of rat. Biochim Biophys Acta 943:419–427
15. Garcia-Calvo M, Knaus H-G, McManus OB, Giangiacomo KM, Kaczorowski GJ, Garcia ML (1994) Purification and reconstitution of the high-conductance calcium-activated potassium channel from tracheal smooth muscle. J Biol Chem 269:676–682
16. Glavinovic MI, Trifaró JM (1988) Quinine blockade of currents through Ca^{2+}-activated K^+ channels in bovine chromaffin cells. J Physiol (Lond) 399:139–152

17. Gola M, Niel JP, Bessone R, Fayolle R (1992) Single channel and whole-cell recordings from non dissociated sympathetic neurons in rabbit coeliac ganglia. J Neurosci Methods 43:13–22
18. Hamill OP, Marty A, Neher E, Sakmann B, Sigworth FJ (1981) Improved patch clamp techniques for high-resolution current recording from cells and cell-free membrane patches. Pflügers Arch 391:85–100
19. Jobling P, McLachlan EM, Sah P (1993) Calcium induced calcium release is involved in the afterhyperpolarization in one class of guinea pig sympathetic neurone. J Auton Nerv Syst 42:251–258
20. Kaczorowski GJ, Knaus H-G, Leonhard RJ, McManus OB, Garcia ML (1996) High conductance calcium-activated potassium channels: Structure, pharmacology, and function. J Bioenerg Biomembr 28:255–267
21. MacKinnon R, Miller C (1988) Mechanism of charybdotoxin block of Ca^{2+}-activated K^+ channels. J Gen Physiol 91:335–349
22. Marrion NV, Tavalin SJ (1998) Selective activation of Ca^{2+}-activated K^+ channels by co-localized Ca^{2+} channels in hippocampal neurons. Nature 395:900–905
23. Marsh SJ, Brown DA (1991) Potassium currents contributing to action potential repolarization in dissociated cultured rat superior cervical sympathetic neurones. Neurosci Lett 133:298–302
24. Marty A (1981) Ca-dependent K channels with large unitary conductance in chromaffin cell membranes. Nature 291:179–181
25. McManus OB, Blatz AL, Magleby KL (1987) Sampling, log binning, fitting, and plotting durations of open and shut intervals from single channels and the effects of noise. Pflügers Arch 410:530–553
26. McManus OB, Helms LM, Pallanck L, Ganetzky B, Swanson R, Leonard RJ (1995) Functional role of the beta subunit of high conductance calcium-activated potassium channels. Neuron 14:645–650
27. McManus OB, Magleby KL (1988) Kinetic states and modes of single large-conductance calcium-activated potassium channels in cultured rat skeletal muscle. J Physiol (Lond) 402: 79–120
28. Miller C, Moczydlowski E, Latorre R, Phillips M (1985) Charybodotoxin, a protein inhibitor of single Ca^{2+}-activated K^+ channels from mammalian skeletal muscle. Nature 313: 316–318
29. Moyer JR, Thompson LT, Black JP, Disterhoft JF (1992) Nimodipine increases excitability of rabbit CA1 pyramidal neurons in an age- and concentration-dependent manner. J Neurophysiol 68:2100–2109
30. Muñoz A, García L, Guerrero-Hernández A (1998) In situ characterization of the Ca^{2+} sensitivity of large conductance Ca^{2+}-activated K^+ channels: implications for their use as near-membrane Ca^{2+} indicators in smooth muscle cells. Biophys J 75:1774–1782
31. Nimigean CM, Magleby KL (1999) The β subunit increases the Ca^{2+} sensitivity of large conductance Ca^{2+}-activated potassium channels by retaining the gating in the bursting states. J Gen Physiol 113:425–440
32. Pardo LA, Heinemann SH, Terlau H, Ludewig U, Lorra C, Pongs O, Stuehmer W (1992) Extracellular K^+ specifically modulates a rat brain K^+ channel. Proc Natl Acad Sci USA 89:2466–2570
33. Pineda JC, Waters RS, Foehring RC (1998) Specificity in the interaction of HVA Ca^{2+} channel types with Ca^{2+}-dependent AHPs and firing behavior in neocortical pyramidal neurons. J Neurophysiol 79:2522–2534
34. Robitaille R, Garcia ML, Kaczorowski GJ, Charlton MP (1993) Functional colocalization of calcium and calcium-gated potassium channels in control of transmitter release. Neuron 11:645–655
35. Sacchi O, Rossi ML, Canella R (1995) The slow Ca^{2+}-activated K^+ current, I_{AHP}, in the rat sympathetic neurone. J Physiol (Lond) 483:15–27
36. Safronov BV, Vogel W (1998) Large conductance Ca^{2+}-activated K^+ channels in the soma of rat motoneurones. J Membr Biol 162:9–15
37. Sah P (1996) Ca^{2+}-activated K^+ currents in neurones: types, physiological roles and modulation. Trends Neurosci 19:150–154
38. Sakmann B, Neher E (1995) Geometric parameters of pipettes and membrane patches. In: Sakmann B, Neher E (eds) Single channel recording, 2nd edn. Plenum, New York, pp 637–650
39. Schreiber M, Yuan L, Salkoff L (1999) Transplantable sites confer calcium sensitivity to BK channels. Nature Neurosci 2:416–421
40. Selyanko AA (1992) Membrane properties and firing characteristics of rat cardiac neurons in vitro. J Auton Nerv Syst 39:198–190
41. Smart TG (1987) Single calcium-activated potassium channels recorded from cultured rat sympathetic neurones. J Physiol (Lond) 389:337–360
42. Trequattrini C, Catacuzzeno L, Petris A, Adams DJ, Franciolini F (1999) Large conductance calcium-activated K channels in rat intracardiac neurons. Pflügers Arch 438:R5
43. Vergara C, Latorre R, Marrion NV, Adelman JP (1998) Calcium-activated potassium channels. Curr Opin Neurobiol 8:321–329
44. Verheugen JA, Vijveberg HPM, Oortgiesen M, Calahan MD (1995) Voltage-gated and Ca^{2+}-activated K^+ channels in intact human T lymphocytes. Noninvasive measurements of membrane currents, membrane potential and intracellular calcium. J Gen Physiol 105:765–794
45. Xi-Moy SX, Dun NJ (1995) Potassium currents in adult rat intracardiac neurones. J Physiol (Lond) 486:15–31
46. Xu Z-J, Adams DJ (1992) Resting membrane potential and potassium currents in cultured parasympathetic neurones from rat intracardiac ganglia. J Physiol (Lond) 456:405–424
47. Yellen G (1984) Ionic permeation and blockade in Ca^{2+}-activated K^+ channels of bovine chromaffin cells. J Gen Physiol 84:157–186